

# CHEM MED CHEM

CHEMISTRY ENABLING DRUG DISCOVERY

## Accepted Article

**Title:** Efficacious doxorubicin delivery using glutathione responsive hollow non-phospholipid vesicles bearing lipoyl cholesterols

**Authors:** Krishan Kumar, Lalit Yadav, Paturu Kondaiah, and Sandeep Chaudhary

This manuscript has been accepted after peer review and appears as an Accepted Article online prior to editing, proofing, and formal publication of the final Version of Record (VoR). This work is currently citable by using the Digital Object Identifier (DOI) given below. The VoR will be published online in Early View as soon as possible and may be different to this Accepted Article as a result of editing. Readers should obtain the VoR from the journal website shown below when it is published to ensure accuracy of information. The authors are responsible for the content of this Accepted Article.

**To be cited as:** *ChemMedChem* 10.1002/cmdc.201900335

**Link to VoR:** <http://dx.doi.org/10.1002/cmdc.201900335>

WILEY-VCH

[www.chemmedchem.org](http://www.chemmedchem.org)

A Journal of



# Efficacious doxorubicin delivery using glutathione responsive hollow non-phospholipid vesicles bearing lipoyl cholesterol

Krishan Kumar,<sup>[a]</sup> Lalit Yadav,<sup>[a]</sup> Paturu Kondaiah,<sup>\*[b]</sup> and Sandeep Chaudhary<sup>\*[a]</sup>

Dedication ((optional))

**Abstract:** Herein, we have developed redox sensitive vesicles using synthesized lipoyl cholesterol and non-ionic surfactant along with optimum level of free cholesterol. Interestingly, a concentration dependent self-assembling behavior was noticed wherein vesicles manifested as hollow spherical (0.15  $\mu\text{M}$ ) and triangular (0.50  $\mu\text{M}$ ) aggregates as observed under scanning electron microscopic (SEM) analysis. The redox responsive characteristic was probed in the presence of dithiothreitol (DTT) which demonstrated a clear increase in size as observed under dynamic light scattering (DLS) measurements. These vesicles could easily encapsulate an anticancer drug, doxorubicin and observed to be adequately stable in the presence of serum. It showed a substantial release of the drug in response to biologically relevant stimulus, *i.e.*, glutathione (GSH). Their toxicity assessment on HeLa and HepG2 cancer cells demonstrated a comparable activity to that of free drug whereas noticeable toxicity enhancement and apoptotic induction were observed against drug resistant HeLa cells which were interpreted through drug cellular internalization.

## Introduction

The design and development of biocompatible drug delivery systems still remains the promising and leading approach to bring about desirable outcomes in anticancer therapeutics.<sup>[1,2]</sup> Towards achieving the therapeutic goals, the development of bio-responsive nanocarriers that respond to either exogenous (*e.g.*, temperature and magnetic field) or endogenous (*e.g.*, pH and redox potential) stimulus has been rigorously exercised in full capacity over the last ten years.<sup>[3-5]</sup> The bio-responsive systems have paved the way for their possible exploitation to combat marked issues in anticancer therapy such as inefficient delivery, tumor cell-specific targeting and the development of resistance to chemotherapeutic drugs.<sup>[4,6-8]</sup> The existing plethora of drug transport vehicles is composed of several nano and micro-structured self assemblies of different amphiphilic structures.<sup>[6,9,10]</sup> The liposomes,<sup>[11]</sup> niosomes,<sup>[12]</sup> micelles,<sup>[13]</sup> nano/micro particles,<sup>[14]</sup> polymersomes<sup>[15]</sup> and nanogels<sup>[16]</sup> are

notable drug delivery systems that have been part of extensive drug delivery research in the hope of achieving desirable outcomes in chemotherapeutic treatments. Significant efforts have been made in order to make these drug carriers bio-responsive for effective release of the drug.<sup>[3,17]</sup> In particular, the relatively low pH of intracellular compartments (endosomes; pH ~5-6/lysosomes; pH ~4-5) to that of blood plasma (pH ~7.4) has been successfully exploited for the development of pH sensitive nanocarriers.<sup>[3,4,18,19]</sup> These nanocarriers remain stable at physiological pH, but degrade rapidly under mildly acidic environment of endosomal/lysosomal compartments, thereby releasing the encapsulated drug inside the cells.<sup>[20]</sup> Likewise, the equally important and substantially explored disulfide bridge based redox sensitive nanocarriers have been designed to disintegrate in response to the relatively high cytosolic concentration of reducing agent, glutathione (GSH) tripeptide (~2-10 mM) to that of extracellular fluids (~2-10  $\mu\text{M}$ ).<sup>[3,17a,21]</sup> In particular, this biological stimulus is crucial owing to the fact that tumor tissues represent a relative high reducing intracellular environment in comparison to normal tissues which renders an opportunity for tumor specific drug transport.<sup>[17b]</sup> Therefore, we herein have attempted to develop reduction sensitive vesicles which are constructed using non-ionic surfactants and cholesterol-lipoic acid conjugates (lipoyl cholesterol). The non-ionic surfactants (*e.g.*, sorbitan esters (spans) and polyethoxylated sorbitan esters (tweens)) self-assemble in to liposome-like vesicles in an aqueous media which are suitable for the encapsulation of lipophilic and hydrophilic drug molecules in vesicular membrane and within the aqueous core respectively.<sup>[12b,22]</sup> The lower cost and greater stability of self-assemblies (vesicles) of non-ionic surfactants have been in marked contrast to those of phospholipids and offer them as promising alternatives to liposome based systems.<sup>[22b,c]</sup> In addition, these are considered to be biodegradable and non-immunogenic which indicate their safe interaction with biological system and are reckoned to be potential candidate for drug delivery application.<sup>[22c]</sup> The inclusion of biological small molecule, *i.e.*, cholesterol during such vesicle preparation is routinely practiced as it provides stability to vesicles and improves encapsulation efficiency of the drug.<sup>[22b,c,23]</sup> Additionally, ethoxylate derivative of cholesterol and other conjugates have also been reported to result in the formation of vesicular structures.<sup>[24]</sup> Therefore, bioconjugates of cholesterol with lipoic acid linked through oxyethylene spacer groups have been synthesized in the current study to blend in with non-ionic surfactant (Figure 1). Lipoic acid is a naturally occurring powerful antioxidant and has been assessed to be reliably safe for human use.<sup>[25]</sup> Thus, it has been approved as an ingredient in many dietary and pharmaceutical supplements. The disulfide linkage of the dithiolane ring in lipoic acid structure is favourably prone to rapid cleavage by cytosolic glutathione of cells and

[a] Dr. K. Kumar, L. Yadav, Dr. S. Chaudhary  
Department of Chemistry  
Malaviya National Institute of Technology  
Jawaharlal Nehru Marg, Jaipur-302017, India  
E-mail: [schaudhary.chy@mnit.ac.in](mailto:schaudhary.chy@mnit.ac.in)

[b] Prof. P. Kondaiah  
Department of Molecular Reproduction, Development and Genetics  
Indian Institute of Science  
Bangalore- 560012, India.  
E-mail: [paturu@iisc.ac.in](mailto:paturu@iisc.ac.in)

Supporting information for this article is given via a link at the end of the document.((Please delete this text if not appropriate))

therefore can be exploited to impart redox sensitivity to drug delivery systems.<sup>[26]</sup> Herein, the non-phospholipid vesicles of polysorbate 20 (Tween 20) containing lipoyl cholesterol (with varying length of oxyethylene spacer) and optimum level of free cholesterol were thoroughly characterized for size and morphological analysis by means of field emission scanning electron microscopy (FE-SEM), high-resolution transmission electron microscopy (HR-TEM) and atomic force microscopy (AFM) studies. The hydrodynamic diameters and surface charge of vesicles were assessed using dynamic light scattering (DLS) and zeta potential measurements respectively. DLS studies further assisted in redox sensitive assessment of these vesicles in terms of change in size which was induced using non-biological and biological reducing agents, *i.e.*, DTT and GSH respectively. The vesicles could efficiently encapsulate an anticancer drug, doxorubicin (DOX) and demonstrated substantial stability against serum. Triggered drug release was ensured in reducing environment. Flow cytometry and confocal microscopic analysis revealed significant drug release inside DOX sensitive cervical (HeLa) and hepatic (HepG2) cancer cells alike free drug. Interestingly, the vesicle mediated drug transport revealed a significantly increased drug cellular internalization in comparison to that of free drug in DOX resistant HeLa cells (DR-HeLa) which resulted in marked induction of apoptosis (annexin V binding) and reduction of cell viability counts (MTT assay). Summarily, the exploitation of lipoyl-cholesterol bearing non-phospholipid vesicles may offer exciting strategy for safe and bio-responsive drug delivery to cancer cells, especially in the condition of multi-drug resistance.

## Results and Discussion

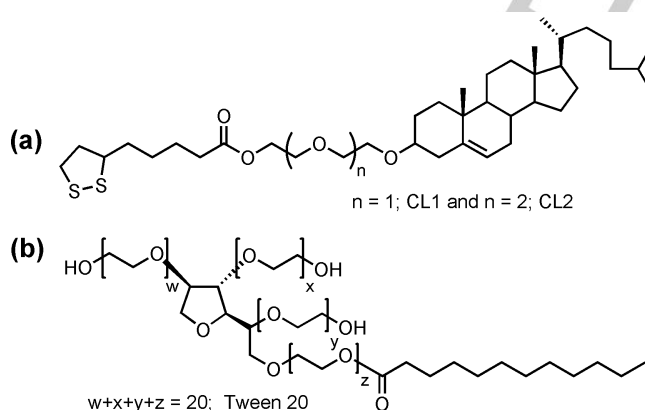
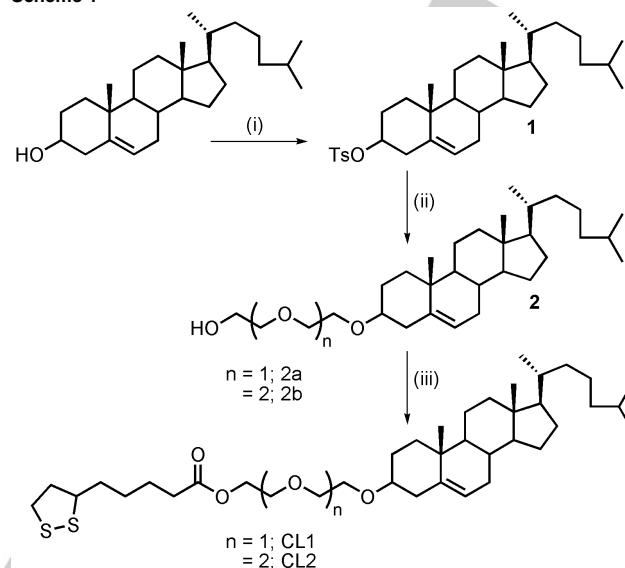


**Figure 1.** Molecular structure of (a) cholesteryl-lipoic acid (CL) conjugates and (b) Tween 20.

**Synthesis of lipoyl-cholesterols.** The lipoylated conjugates of cholesterol were prepared as summarized in Scheme 1.<sup>[27]</sup> Briefly, cholesteryl tosylate (1) was reacted with diethylene glycol and triethylene glycol to give rise to diethoxy (2a) and triethoxy cholesterol (2b) derivatives respectively which were then coupled to lipoic acid using DCC based esterification procedure to obtain CL1 and CL2 conjugates. The details of

synthesis procedures and characterizations have been placed in Supporting Information.

**Scheme 1<sup>a</sup>**



<sup>a</sup>Reagents and conditions: i) *p*-TsCl/Py/DCM, rt, 20 h, 80%; ii) di-/tri-ethylene glycol, 1,4-dioxane, 110 °C, 6 h, 65%/62%; iii) Lipoic acid, DCC, DMAP (cat), DCM, 6 h, rt, 70%/80%.

**Preparation and characterization of vesicles.** Non-ionic surfactants are the preferred surface active agents for the preparation of low cost non-phospholipid based vesicular structures. The stability and benign hemolytic behaviour of these vesicles remark them to be superordinate to other vesicle forming amphiphiles.<sup>[22,28]</sup> Similar to liposome organization, non-ionic surfactants vesicles are produced from amphiphiles with hydrophilic head and hydrophobic tail. The popularly known series of surfactants, *i.e.*, Tweens which bear a long alkyl chain as well as a large hydrophilic moiety are approved pharmaceutical excipients and known to give rise to stable vesicular structures when co-formulated with cholesterol in an aqueous phase.<sup>[22c,28]</sup> These structures are termed as niosomes and have been reported to enable the entrapment of both hydrophilic and lipophilic drugs. Having realized the role of cholesterol in such vesicular structure preparation, we co-formulated Tween 20 (polysorbate type non-ionic surfactant) with cholesteryl-lipoic acid conjugates (CL1 and CL2) synthesized in the present study (Figure 1) to give rise to redox sensitive vesicles. The disulfide bond of lipoic acid is rapidly cleaved in the presence of adequate reducing environment and triggers the disorganization of self-assembled aggregates which is considered advantageous for the release of entrapped cargoes.<sup>[26]</sup> Therefore the proportions of CL1/CL2 bioconjugates and free cholesterol in vesicle composition were first optimized (Table S1) based on the response to non biological reducing agent, dithiothreitol (DTT; 10 mM) to mimic the intracellular

reductive environment and size of the vesicles using dynamic light scattering (DLS) measurements. The thin-film hydration method was employed for the preparation of vesicles. The resulting vesicle dispersions were appropriately diluted and their hydrodynamic diameters were determined with and without DTT treatment (10 mM; 4 h). The vesicle composition, i.e., T20/cholesterol/CL; 15/5.0/10 for both CL1 and CL2 containing vesicles, termed herein as CL1V and CL2V respectively, was sorted by its optimal response to DTT treatment and appropriate size (Table S1). The average hydrodynamic diameters of both CL1V and CL2V ranged between 120 nm and 130 nm. Additionally, the DLS measurements exhibited low polydispersity index (PDI) values (<0.25) for both vesicle preparations (Table S1) which suggested nearly monodisperse population of vesicles.<sup>[29]</sup> Notably, the variation in proportions of cholesterol and CL conjugates in different vesicle compositions did not evidence any significant change in the size of vesicles. The zeta potential measurements revealed that the surface charges of the CL1V and CL2V were  $\sim$ -37 and  $\sim$ -40 mV which indicated the adequate stability of these formulations due to electrostatic stabilization of the particles (Figure S1).<sup>[30]</sup> The DTT treatment of these vesicles led to an evident increase in their hydrodynamic diameters (>350 nm) and PDI values (>0.60) which suggested the triggered disorganization of vesicular self assembly owing to redox sensitivity of disulphides of lipoyl units.<sup>[31]</sup> The representative DLS graph depicting the change in size of CL1V after treatment with DTT has also been shown in comparison to that of without DTT treatment (Figure S2a and S2b).

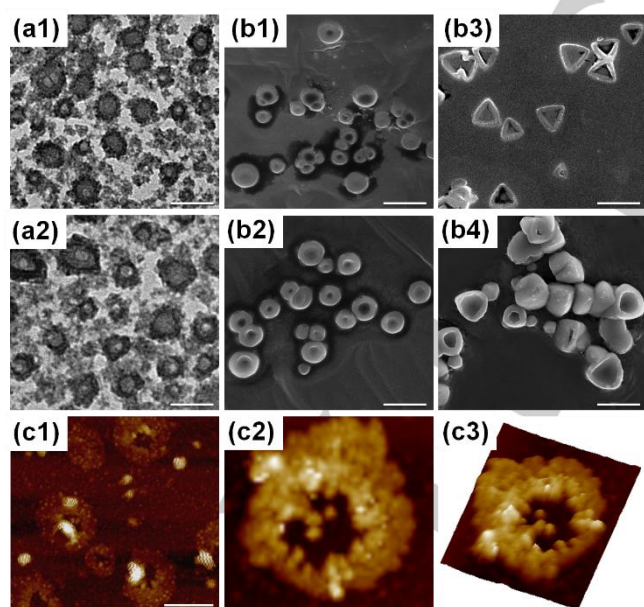


**Figure 2.** The morphological investigation of CL1V (a1, b1 and b3) and CL2V (a2, b2 and b4) using TEM (a1 and a2) and SEM (b1-b4) at concentrations 0.15 mM (a1, a2, b1 and b2) and 0.50 mM (b3 and b4). The AFM visualization of CL2V structure (c1) along with 2D (c2) and 3D (c3) representation of a single CL2V vesicle. Scale bar = 100 nm (TEM) and 200 nm (SEM and AFM).

The CL1V and CL2V were further subjected to Transmission electron microscopic (TEM) analysis for their morphological investigation. It revealed the vesicles to be hollow in nature with spherical morphology (Figure 2a1 and 2a2). Further imaging of vesicles through scanning electron microscope (SEM) demonstrated the presence of hollow spherical structures which corroborated the observations under TEM analysis (Figure 2b1 and 2b2). Interestingly, different morphological feature was revealed by the vesicles at relatively low dilution wherein at concentration  $\geq$ 0.5 mM, it manifested as triangular structures with relatively deep and prominent cavities like that of a bowl as shown in Figure 2b3 and 2b4.<sup>[32]</sup> The triangular vesicles appeared to be relatively bigger in size than the spherical vesicles. The surface morphological characteristic of the vesicles was further assessed by means of atomic force microscopy (AFM). The AFM imaging (Figure 2c1-2c3) further substantiated the presence of hollow structures which appeared like multicellular vesicles.<sup>[33]</sup> Such hollow structured self-assemblies have been reported to be of great interest because of their high drug encapsulation efficiency (EE) and an efficient or complete drug release.<sup>[34]</sup>

**Drug encapsulation and release.** The optimized formulations were further investigated for their drug encapsulation efficacy to profile their possible exploitation as redox sensitive drug delivery vesicles for the rapid release of drug upon exposure to cell reducing environments. The routinely prescribed chemotherapy medication, doxorubicin was encapsulated in CL1V and CL2V and the encapsulation efficiencies (EE) were observed to be 55.89% and 56.76% respectively as determined by the calibration plot of doxorubicin. The drug delivery systems should be adequately stable in the blood circulation and should not exhibit premature drug release.<sup>[17a]</sup> Therefore, we subsequently assessed the stability of doxorubicin loaded vesicles (CL1V-DOX and CL2V-DOX) in the presence of 10% serum condition (fetal bovine serum; FBS).

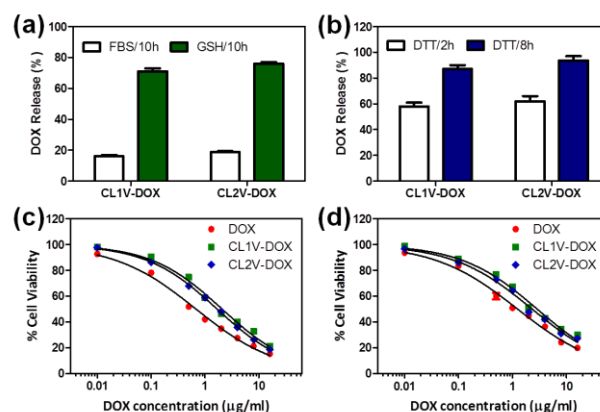


**Figure 3.** Evaluation of the stability of CL1V-DOX and CL2V-DOX against serum (FBS; 10%) treatment and redox sensitivity against glutathione (GSH; 10 mM) treatment (a). Dithiothreitol (DTT; 10 mM) mediated drug release from vesicles at different time points (b). Cytotoxicity analysis of CL1V-DOX and CL2V-DOX against HeLa (c) and HepG2 (d) cells in comparison with free drug 48 h post treatment.



It was noticed that none of the CL1V-DOX and CL2V-DOX showed any substantial loss of encapsulated doxorubicin. The presence of serum could induce only ~16% and ~19% release of the drug after 10 h incubation period (Figure 3a) which deduced the stability of these vesicles. On the other hand, rapid and significant drug release was observed from the vesicles (0.15 mM) in the presence of DTT (10 mM) when ascertained at two different time points (2 h and 8 h). The DTT induced release of >50% of the encapsulated drug within 2 h (Figure 3b). We also probed the reduction induced drug release behaviour in the presence of biological reducing agent, glutathione (GSH; 10 mM) which evidenced ~70% release of DOX after 10 h incubation period (Figure 3a). In order to look into drug release behaviour from different morphologies (as observed under SEM), we also measured the amount of released drug at relatively low dilution (0.50 mM) of vesicles wherein it appeared as triangular hollow structures. The DTT treatment (2 h) resulted in a relatively more prominent drug release (~80%) which suggested the practical utility of structurally distinct morphologies (Figure S3). The observations herein concluded that these vesicles are significantly stable in physiological condition and can cause to rapid release of encapsulated drug in the presence of intracellular stimulus (redox potential).<sup>[21a]</sup>

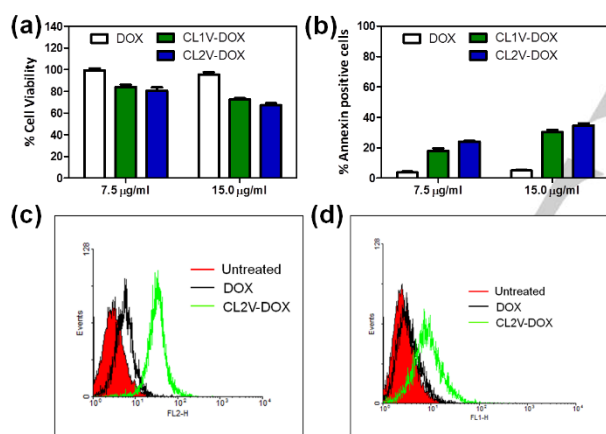


**Figure 4.** Cytotoxicity (a) and annexin V binding analysis (b) of CL1V-DOX and CL2V-DOX treated DR-HeLa cells in comparison with free DOX at 96 h and 72 h post treatment respectively. Representative overlaid flow cytometry histograms for the (c) comparative cellular internalization of drug (7.5 µg/ml; 4h) and (d) annexin V-FITC binding between free DOX and CL2V-DOX mediated treatments (15 µg/ml; 72h).

**Cytotoxicity and cellular internalization of CL1V-DOX and CL2V-DOX.** Reduction triggered intracellular drug release from nanocarriers has been realized as potential strategy to achieve improved anticancer therapeutics.<sup>[21]</sup> Hence, there is a growing need to develop such responsive and safe nanocarriers for efficacious drug delivery to reach therapeutic level of the drugs. We therefore determined the cytotoxicity of CL1V-DOX and CL2V-DOX formulations against cervical cancer (HeLa) cells and human liver carcinoma (HepG2) cells in comparison with free drug for a 48 h treatment following the conventional MTT

based assay (Figure 3c and 3d). It exhibited that both the formulations significantly reduced the cell viability counts in both the cell lines and the observed IC<sub>50</sub> values for CL1V-DOX (2.07 µg/ml; HeLa and 2.86 µg/ml; HepG2) and CL2V-DOX (1.67 µg/ml; HeLa and 2.30 µg/ml; HepG2) were comparable to that of free doxorubicin treatment (0.68 µg/ml; HeLa and 1.24 µg/ml; HepG2). Notably, the respective concentrations of blank vesicles (CL1V and CL2V) did not show any cytotoxic response to either of the cell lines studied (Figure S4). This in turn substantiated the non-toxic nature of non-ionic surfactant based formulations blended with CL conjugates which make them preferred tool for various delivery applications.<sup>[28b]</sup> In addition, we examined the cytotoxicity of CL1V/CL2V-DOX vesicles against non-cancerous fibroblast cells, NIH3T3. Interestingly, it revealed significantly high cell viability counts for vesicle mediated DOX treatments when compared to that of free DOX treatment (Figure S5). This in turn signified that these formulations could be promising candidates for receptor-targeted drug delivery application.

The emergence of drug resistance during chemotherapy treatments has been reported as a vital issue against successful therapeutics.<sup>[35a]</sup> The chemotherapeutics under such condition go with additional and/or frequent drug doses which develop serious side effects and consequently leads to possible treatment failure.<sup>[35b]</sup> The stimuli responsive drug delivery systems have been ensured to raise the intracellular accumulation of drugs in vitro for reaching the therapeutic levels in prospect towards overcoming the drug resistance.<sup>[8,11a,20a,35]</sup>

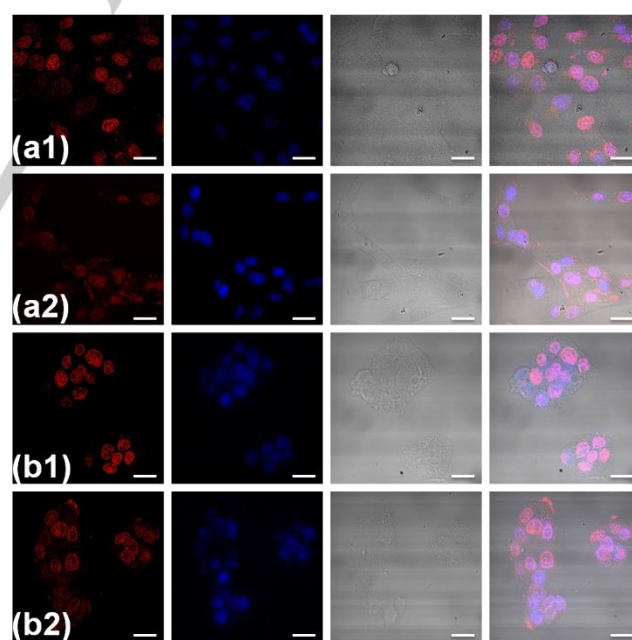


**Figure 5.** The confocal microscopic investigation of DOX cellular internalization in HeLa (a1 and a2) and HepG2 (b1 and b2) cells after treatment with free DOX (a1 and b1) and CL2V-DOX (a2 and b2) at the concentration of 5 µg/ml for 4 h. Each panel, respectively, left to right annotates DOX fluorescence, DAPI (nuclear stain) fluorescence, bright field image and overlay of previous three images. Scale bar = 20 µm.

We therefore examined the cytotoxic effect of CL1V-DOX and CL2V-DOX against doxorubicin resistant HeLa cells (DR-HeLa).<sup>[20a]</sup> Owing to significant DOX resistance ( $IC_{50}$ ; 61.45  $\mu$ g/ml) of DR-HeLa cells (Figure S6), we refrained from determination of  $IC_{50}$  values for CL1V-DOX and CL2V-DOX because it would require relatively high concentration of vesicles for equivalent DOX concentration that exert potential cytotoxic effects in vitro pertaining to the concentration of Tween type surfactant (Figure S4).<sup>[36]</sup> Therefore, we checked out the cell viability only at 7.5 and 15  $\mu$ g/ml. Interestingly, in DR-HeLa cells a marked difference in cell viabilities was observed between vesicle mediated DOX treatments and that of free drug. As shown in Figure 4a, the CL1V-DOX mediated treatments resulted in ~17 and ~28 % cell death at 7.5 and 15.0  $\mu$ g/ml, respectively, 96 h post treatment. At these concentrations the observed cell death for CL2V-DOX treatment was ~20 and 34%. However, no significant decrease in cell viability counts was detected for free doxorubicin treatment of DR-HeLa cells.

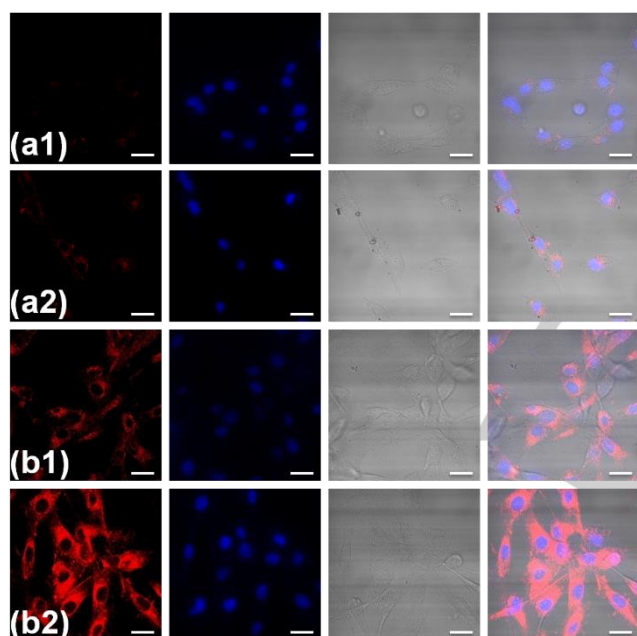


**Figure 6.** The confocal microscopic investigation of DOX cellular internalization in DR-HeLa cells after treatment with free DOX (a1 and b1) and CL2V-DOX (a2 and b2) at the concentration of 15  $\mu$ g/ml for the periods of 4 h (a1 and a2) and 24 h (b1 and b2). Each panel, respectively, left to right annotates DOX fluorescence, DAPI (nuclear stain) fluorescence, bright field image and overlay of previous three images. Scale bar = 20  $\mu$ m.

This distinct cytotoxic response of vesicle mediated DOX treatment was also evaluated in terms of monitoring apoptotic DR-HeLa cell population following annexin-V binding assay using flow cytometry. In apoptotic cells, the phosphatidylserine appears on the cell membrane surface and can easily be detected using fluorophore bound annexin-V which is in turn used for quantitative determination of apoptosis.<sup>[37]</sup> The annexin-V FITC labelling of free DOX treated DR-HeLa cells did not

reveal any notable apoptotic induction (~4%) whereas significant apoptosis (~35% annexin-V positive cells) was detected for CL2V-DOX mediated treatment (Figure 4b and 4d). The observation clearly evidenced the efficacious cellular transport of DOX through vesicles across the membrane of DOX resistant HeLa cells which resulted in induction of apoptosis and thereby cell death.

The study was then further advanced while looking into comparative cellular internalization of drug in HeLa and DR-HeLa cells for the treatments mediated by CL1V-DOX/CL2V-DOX and free DOX by means of flow cytometry and confocal microscopy experimentation. The quantitative analysis of flow cytometry results revealed that CL1V-DOX and CL2V-DOX mediated treatment showed nearly similar DOX fluorescence intensity to that of free drug mediated treatment in HeLa cells (Figure S7). The confocal microscopic analysis revealed substantial DOX fluorescence in the cell nuclei (of both HeLa and HepG2 cells) for CL1V/CL2V mediated DOX treatments which indicated rapid and efficient drug release from the vesicles. This was evident from the observed magenta colour in merged images as a result of co-localization of DOX (red) and DAPI (nuclear stain; blue) as shown in Figure 5.<sup>[12b]</sup> Such efficacious nuclear distribution of drugs has always been desirable in the case of nanocarrier/nanoparticle mediated drug delivery.<sup>[20a]</sup> In addition, the quantitative analysis of cellular DOX fluorescence in confocal micrographs further substantiated the results of flow cytometry (Figure S8). In case of DR-HeLa cells, significantly enhanced cellular DOX internalization manifested for CL1V-DOX and CL2V-DOX treatments in comparison to that of free DOX as evidenced from the stark difference in quantitative analysis of DOX fluorescence intensity using flow cytometry (Figure 4c and S9). The confocal microscopic analysis corroborated the observation as CL1V-DOX and CL2V-DOX treated (24 h; 15  $\mu$ g/ml) DR-HeLa cells exhibited much brighter DOX fluorescence than those treated with free drug (Figure 6b1 and 6b2). This enhancement in cellular DOX fluorescence was also quantified from the micrographs of three independent experiments which demonstrated almost doubled mean fluorescence intensity of DOX in DR-HeLa Cells treated with vesicles (Figure S10). This distinct activity of drug loaded vesicles in DR-HeLa cells was also evaluated 4 h post treatment and it was observed that CL1V/CL2V-DOX treatment led to a clearly visible intracellular DOX fluorescence whereas free drug treatment did not reveal any noticeable DOX fluorescence inside the cells (Figure 6a1 and 6a2).<sup>[38]</sup> This can be plausibly ascribed to the ability of nanocarriers to bypass the drug efflux pumps on the membrane of drug resistant cells which results in the increased intracellular concentration of drug.<sup>[7,38]</sup> The drug internalization study also helped in understanding the observed cytotoxicity profile against both drug sensitive and resistant cancer cells which apparently relied upon the delivered intracellular concentration of drug.<sup>[20a,38]</sup> Based on these observations, it can be suggested that the lipoyl cholesterol could be exploited to give rise to redox sensitive vesicles which possess excellent potential of being examined as drug delivery vehicle, especially in the case of drug resistance. In addition, the idea of functionalizing these vesicles further for site-specific drug delivery would be highly advantageous as it

may derive pharmacologically effective formulations. The development of such bioconjugates promises an outright application to be blended in different liposomal and/or niosomal formulation with various other amphiphilic components to obtain biocompatible and bioresponsive delivery vehicles.

## Conclusions

Summarily, two bioconjugates (lipoyl-cholesterols) which differ in terms of the length of oxyethylene spacer  $[-OCH_2(-CH_2-O-CH_2-)_nCH_2O-]$ ;  $n = 1$  and  $2$ ] have been successfully synthesized and exploited as the biocompatible component in the fabrication of reduction responsive non-phospholipid vesicles. The optimized formulations (Tween 20/cholesterol/CL; 15/5.0/10) were thoroughly characterized by means of HR-TEM, FE-SEM, and AFM. Self-assembled hollow structures (vesicles) of triangular shape were observed at  $\geq 0.5$  mM concentration, however, below which (0.1 mM) it appeared to be spherical in morphology. The polydispersity distribution index (PDI) values ( $< 0.25$ ) in DLS measurements suggested a nearly monodisperse vesicle population. Zeta potential measurements revealed a strongly negative surface charge ( $> 30$ ) in favour of the stability of the vesicles. The vesicles could encapsulate chemotherapeutic drug, doxorubicin efficiently (%EE;  $> 55\%$ ) and showed adequate response to reducing environment (DTT and GSH) to release the encapsulated drug. The MTT based cytotoxicity studies revealed that vesicle mediated drug treatment had comparable  $IC_{50}$  values to that of free drug against HeLa and HepG2 cells. On the other hand, it demonstrated a significant decrease in cell viability counts against doxorubicin resistant HeLa (DR-HeLa) cells when compared to free drug treatments. Flow cytometric and confocal microscopic analysis further evidenced in favour of cytotoxicity profile wherein it demonstrated alike cellular fluorescence of doxorubicin in doxorubicin sensitive HeLa and HepG2 cells for both the treatments mediated by either free drug or via vesicles. However, significantly higher doxorubicin fluorescence was noticed in DR-HeLa cells for vesicle mediated treatment in comparison to free drug which resulted in notable induction of apoptosis and cell death as observed in annexin V binding and MTT assay respectively. Concisely, these lipoyl cholesterol based reduction responsive bioconjugates offer a viable means of developing different surfactant or liposome based vesicles which can be exploited as promising candidates to improve the efficacy of chemotherapeutic treatments especially in drug-resistant carcinomas.

## Experimental Section

**Materials.** Analytical grade reagents and solvents were procured from best-known sources and were used as received. Cholesterol, Lipic acid and DAPI, MTT reagent, DMSO, Tween 20 and silica gel (mesh size; 60–120) were purchased from Merck. Di-/tri-ethylene glycol, DCC reagent and DMAP were purchased from Spectrochem Pvt. Ltd. Dulbecco's modified Eagle's medium (DMEM), Dulbecco's phosphate buffered saline

(DPBS), Gibco fetal bovine serum (FBS) and annexin V- FITC conjugate were received from Thermo Fisher Scientific.

**Synthesis of lipoyl cholesterol.** The details of the synthetic procedures for lipoylated cholesterol derivatives have been given in Supporting Information. All compounds were fully characterized by  $^1H$  NMR,  $^{13}C$  NMR and HR-MS.  $^1H$  NMR spectra of compounds were recorded on an ECS 400 MHz (JEOL) NMR spectrometer and  $^{13}C$  NMR were recorded at 100 MHz. Mass spectra were recorded on a Xevo G2-S Q ToF (Waters, USA).

**Preparation and characterization of vesicles.** A lipid layer hydration method was employed for the preparation of vesicles wherein Tween 20 and different proportions of CL1 and CL2 along with cholesterol were dissolved in chloroform:methanol and evaporated under reduced pressure to produce a thin lipid film on the wall of a round-bottomed flask. The film was then hydrated with sterile milli-Q water followed by vortex mixing for 20 min and bath sonication at  $60^\circ C$  for 15 min. The suspensions were diluted hundred times and subjected to size and morphological analysis using Tecnai G2 20 (FEI) S-Twin transmission electron microscope (TEM) and Nova Nano FE-SEM 450 (FEI) scanning electron microscope (SEM). For TEM; samples were placed on carbon coated copper grid and negatively stained using 2% phosphotungstic acid (PTA) solution before imaging. For SEM; samples were loaded on carbon conductive adhesive tape placed on stubs and sputter coated using gold before imaging. The AFM imaging was performed using a multimode scanning probe microscope (Bruker). The size distributions {dynamic light scattering (DLS) measurements} of different vesicle suspension before and after DTT treatment and zeta potentials were analyzed on Zetasizer Nano from Malvern Instruments.

**Drug encapsulation and release studies.** The drug, doxorubicin hydrochloride (4.0 mg/ml) was added to optimized formulations of CL1V and CL2V during hydration step and thereafter followed the same procedure as discussed above. The untrapped drug was removed by centrifugation and the % entrapment was calculated by means of recording UV/Vis spectrum of the supernatant drug molecules ( $\lambda_{max}$ ; 485 nm) on a LAMBDA 750 (Perkin Elmer) UV/Vis NIR Spectrophotometer as follows.  $\%EE = (A_v/A_t) \times 100$ ;  $A_v$  = absorbance of vesicle entrapped drug =  $A_t - A_s$ ;  $A_t$  and  $A_s$  = absorbance of total drug and that of supernatant. Thereafter, the amount of vesicle entrapped drug was calculated using a standard calibration plot of drug. To examine drug release, CL1V and CL2V suspension were added to buffer solution (10 mM; pH = 7.4) and treated with serum (FBS; 10%), GSH (10 mM) and DTT (10 mM). Thereafter extent of drug release (R) was evaluated at desirable time points by means of UV/Vis spectrophotometer using following formula.  $\%R = (A_t - A_0 / A_{100} - A_0) \times 100$  where  $A_0$  is the initial absorbance,  $A_t$  is the absorbance at set time points post treatment and  $A_{100}$  represents absorbance of samples with complete drug leakage in the presence of isopropanol.

**Cytotoxicity analysis.** The cytotoxicity for blank and DOX encapsulated CL1V and CL2V in comparison with free DOX was determined using MTT based colorimetric assay against human liver carcinoma cell line (HepG2 cells), human cervical cancer cell line (HeLa cells) and DOX resistant culture of HeLa cells (DR-HeLa cells). The cells were plated in a 96-well cell culture plate (HepG2/HeLa;  $1 \times 10^4$  cells/well and DR-HeLa;  $5 \times 10^3$  cells/well) in cell culture medium, Dulbecco's Modified Eagle medium (DMEM) supplemented with 10% serum (FBS). After 24 h, cells were treated with CL1V/CL2V and their DOX containing formulations along with free DOX at different drug concentrations in 200  $\mu L$  of cell culture medium and placed in an incubator set at  $37^\circ C$  and supplied with 5%  $CO_2$ , for a period of 48 h (HepG2 and HeLa) and 96 h (DR-HeLa). Then, 20  $\mu L$  of MTT (3-(4,5-dimethylthiazol-2-yl)-2,5-diphenyl



tetrazoliumbromide) reagent {stock; 5.0 mg/mL in DPBS (Dulbecco's Phosphate-Buffered Saline)} was added for 4 h. Thereafter entire medium was carefully aspirated, and DMSO (200  $\mu$ L) was added to the wells. The absorbance was measured using a microplate reader (570 nm). Three such independent treatment procedures including triplicates of all the concentrations were employed for the determination of IC<sub>50</sub> values following an analysis under Graphpad Prism software with nonlinear regression model {log (inhibitor) versus response; variable slope}.

**Flow cytometry analysis.** The cellular internalization of free DOX and CL1V-DOX/CL2V2-DOX was evaluated by means of flow cytometry. In a typical experiment, cells ( $5 \times 10^4$  cells/well) were seeded in a 24 well plate and treated with desired formulations at desired concentrations and time points 24 h post cell seeding. After treatment, the media was carefully aspirated from wells and the cells were washed with DPBS and harvested in 500  $\mu$ L of DPBS supplemented with 0.1 % FBS following trypsinization. The DOX fluorescence intensity in cell samples was then analyzed on a flow cytometer (BD FACSCalibur™, BD Biosciences, USA) wherein untreated cells served as control. The results obtained with flow cytometer were analyzed using WinMDI 2.9 software and represented as geometric mean of fluorescence intensity (GMFI). For the quantitative determination of apoptotic DR-HeLa cell population annexin V-FITC conjugate was used. For which, the manufacturer's protocol was followed wherein untreated DR-HeLa cells and those treated with free DOX and CL2V-DOX were suspended in annexin-binding buffer (10 mM HEPES, 140 mM NaCl, and 2.5 mM CaCl<sub>2</sub>, pH 7.4) provided with the kit. Thereafter, 5  $\mu$ L of the annexin V-FITC conjugate was added to cells for ~10 min and these cell samples were analyzed for quantitative annexin binding using flow cytometry.

**Confocal microscopic analysis.** The HeLa, DR-HeLa and HepG2 cells were seeded on coverslips placed in a 12-well plate at the density of  $1 \times 10^5$  cells/well. After 24 h, cells were incubated with CL1V/CL2V-DOX formulations and free DOX at desired concentrations for desired time points (4 h and 24 h). Thereafter, entire culture medium was carefully removed and the cells were washed three times with DPBS which was then followed by cell fixation using 4% paraformaldehyde solution for 15 min and subsequent wash with DPBS. Then cell nuclei were stained with 4',6-diamidino-2-phenylindole (DAPI) for 10 min. The coverslips were removed from wells and placed on glass slides over antifade mounting medium and imaged using Zeiss LSM 510 Meta Confocal Microscope.

## Acknowledgements

S. C. acknowledges DST, New Delhi for DST-NRF Indo-South Africa Joint Research Project (DST/INT/South Africa/P-19/2016). K.K. acknowledges CSIR, New Delhi for providing financial assistance in the form of research associateship (Award No.: 09/964(0009)2K17). L.Y. thanks DST, New Delhi for senior research fellowship (SRF). Materials Research Centre (MRC), MNIT, Jaipur is gratefully acknowledged for characterization facilities.

**Keywords:** cholesterol bioconjugates • drug delivery • lipolic acid • reduction responsive • vesicles

- [1] C. Y. Ang, S. Y. Tan, Y. Zhao, *Org. Biomol. Chem.* **2014**, *12*, 4776-4806.
- [2] M. C. Garcia, C. Aloisio, R. Onnainty, G. Ullio-Gamboa, Self-assembled nanomaterials, in: R. Narayan (Ed.), *Nanobiomaterials: Nanostructured Materials for Biomedical Applications*, Elsevier BV, 2018, pp. 41-94.
- [3] S. Mura, J. Nicolas, P. Couvreur, *Nat. Mater.* **2013**, *12*, 991-1003.
- [4] M. Overchuk, G. Zheng, *Biomaterials* **2018**, *156*, 217-237.
- [5] L. Li, W. W. Yang, D. G. Xu, *J. Drug Target.* **2019**, *27*, 423-433.
- [6] S. Senapati, A. K. Mahanta, S. Kumar, P. Maiti, *Signal Transduct. Target Ther.* **2018**, *3*, 7.
- [7] Y. Huang, S. P. C. Cole, T. Cai, Y. Cai, *Oncol. Lett.* **2016**, *12*, 11-15.
- [8] S. Wang, P. Huang, X. Chen, *ACS Nano*, **2016**, *10*, 2991-2994.
- [9] G. Verma, P. A. Hassan, *Phys. Chem. Chem. Phys.* **2013**, *15*, 17016-17028.
- [10] P. Davoodi, L. Y. Lee, Q. Xu, V. Sunil, Y. Sun, S. Soh, C. H. Wang, *Adv. Drug Deliv. Rev.* **2018**, *132*, 104-138.
- [11] a) T. Koyanagi, J. L. Cifelli, G. Leriche, D. Onofrei, G. P. Holland, J. Yang, *Bioconjugate Chem.* **2017**, *28*, 2041-2045; b) D. J. Lundy, K. J. Lee, I. C. Peng, C. H. Hsu, J. H. Lin, K. H. Chen, Y. W. Tien, P. C. H. Hsieh, *ACS Nano*, **2019**, *13*, 97-113.
- [12] a) L. Tavano, L. Mauro, G. D. Naimo, L. Bruno, N. Picci, S. Andò, R. Muzzalupo, *Langmuir* **2016**, *32*, 8926-8933; b) S. Naderinezhad, G. Amoabediny, F. Haghiralsadat, *RSC Adv.* **2017**, *7*, 30008- 30019; c) F. Nowrozi, S. Dadashzadeh, H. Soleimanjahi, A. Haeri, S. Shahhosseini, J. Javidi, H. Karimi, *Nanomedicine (Lond)* **2018**, *13*, 2201-2219.
- [13] a) M. Xu, C. Y. Zhang, J. Wu, H. Zhou, R. Bai, Z. Shen, F. Deng, Y. Liu, J. Liu, *ACS Appl. Mater. Interfaces* **2019**, *11*, 5701-5713; b) Z. S. Liao, S. Y. Huang, J. J. Huang, J. K. Chen, A. W. Lee, J. Y. Lai, D. J. Lee, C. C. Cheng, *Biomacromolecules*, **2018**, *19*, 2772-2781.
- [14] a) F. Emami, A. Banstola, A. Vatanara, S. Lee, J. O. Kim, J. H. Jeong, S. Yook, *Mol. Pharmaceutics* **2019**, *16*, 1184-1199; b) A. F. Moreira, D. R. Dias, E. C. Costa, I. J. Correia, *Eur. J. Pharm. Sci.* **2017**, *104*, 42-51.
- [15] F. Oroojalian, M. Babaei, S. M. Taghdisi, K. Abnous, M. Ramezani, M. Alibolandi, *J. Control. Release* **2018**, *288*, 45-61.
- [16] P. Wei, G. Gangapurwala, D. Pretzel, M. N. Leiske, L. Wang, S. Hoepfner, S. Schubert, J. C. Brendel, U. S. Schubert, *Biomacromolecules*, **2019**, *20*, 130-140.
- [17] a) B. Chen, W. Dai, B. He, H. Zhang, X. Wang, Y. Wang, Q. Zhang, *Theranostics* **2017**, *7*, 538-558; b) R. Mo, Z. Gu, *Mater. Today* **2016**, *19*, 274-283; c) H. Zheng, Y. Zhang, L. Liu, W. Wan, P. Guo, A. M. Nystrom, X. Zou, *J. Am. Chem. Soc.* **2016**, *138*, 962-968.
- [18] E. S. Lee, Z. Gao, Y. H. Bae, *J. Control. Release* **2008**, *132*, 164-170.
- [19] H. S. El-Sawy, A. M. Al-Abd, T. A. Ahmed, K. M. El-Say, V. P. Torchilin, *ACS Nano* **2018**, *12*, 10636-10664.
- [20] a) P. Moitra, K. Kumar, P. Kondaiah, S. Bhattacharya, *Angew. Chem. Int. Ed.* **2014**, *53*, 1113-1117; b) J. Seo, J. Lee, C. B. Lee, S. K. Bae, K. Na, *Bioconjugate Chem.* **2019**, *30*, 621-632; c) J. D. Wallat, J. K. Harrison, J. K. Pokorski, *Mol. Pharmaceutics* **2018**, *15*, 2954-2962; d) Z. Liang, Z. Yang, H. Yuan, C. Wang, J. Qi, K. Liu, R. Cao, H. Zheng, *Dalton Trans.* **2018**, *47*, 10223-10228.
- [21] a) L. Ling, M. Ismail, Y. Du, Q. Xia, W. He, C. Yao, X. Li, *Mol. Pharmaceutics* **2018**, *15*, 5479-5492; b) Y. Y. Peng, D. Diaz-Dussan, P. Kumar, R. Narain, *Bioconjugate Chem.* **2019**, *30*, 405-412.
- [22] a) D. A. Selec, M. Selec, F. Stahl, T. Scheper, *RSC Adv.* **2017**, *7*, 33378-33384; b) R. Bartelds, M. H. Nematollahi, T. Pols, M. C. A. Stuart, A. Pardakhty, G. Asadikaram, B. Poolman, *PLoS ONE* **2018**, *13*, e0194179; c) D. A. Selec, M. Selec, J. G. Walter, F. Stahl, T. Scheper, *J. Nanomater.* **2016**, *2016*, Article ID 7372306.
- [23] H. Abdelkader, A. W. G. Alani, R. G. Alany, *Drug Deliv.* **2014**, *21*, 87-100.
- [24] a) K. R. Patel, M. P. Li, J. R. Schuh, J. D. Baldeschwieler, *Biochim. Biophys. Acta* **1984**, *797*, 20-26; b) I. Cho, S. Dong, S. W. Jeong, *Polymer*, **1995**, *36*, 1513-1515.
- [25] a) K. P. Shay, R. F. Moreau, E. J. Smith, A. R. Smith, T. M. Hagen, *Biochim. Biophys. Acta* **2009**, *1790*, 1149-1160; b) D. Tibullo, G. Li Volti, C. Giallongo, S. Grasso, D. Tomassoni, C. D. Anfuso, G. Lupo, F. Amenta, R. Avola, V. Bramanti, *Inflamm. Res.* **2017**, *66*, 947-959.



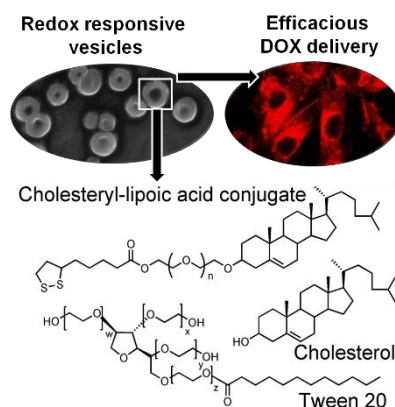
- [26] a) H. Yang, W. Shen, W. Liu, L. Chen, P. Zhang, C. Xiao, X. Chen, *Biomacromolecules* **2018**, *19*, 4492-4503; b) M. Zheng, Y. Zhong, F. Meng, R. Peng, Z. Zhong, *Mol. Pharmaceutics* **2011**, *8*, 2434-2443; c) P. Dharmalingam, B. Marrapu, C. Voshavar, R. Nadella, V. K. Rangasami, R.V. Shaji, S. Abbas, R.B.N. Prasad, S. S. Kaki, S. Marepally, *Colloids Surf. B Biointerfaces* **2017**, *152*, 133-142; d) B. Maiti, K. Kumar, P. Moitra, P. Kondaiah, S. Bhattacharya, *Bioconjugate Chem.* **2018**, *29*, 255-266.
- [27] A. Bajaj, P. Kondiah, S. Bhattacharya, *J. Med. Chem.* **2007**, *50*, 2432-2442.
- [28] a) G. P. Kumar, P. Rajeshwarrao, *Acta Pharm. Sin. B* **2011**, *1*, 208-219; b) X. Ge, M. Wei, S. He, W. E. Yuan, *Pharmaceutics* **2019**, *11*, 55.
- [29] M. Danaei, M. Dehghankhold, S. Ataei, F. H. Davarani, R. Javanmard, A. Dokhani, S. Khorasani, M. R. Mozafari, *Pharmaceutics* **2018**, *10*, 57.
- [30] Z. C. Ertekin, Z. S. Bayindir, N. Yuksel, *Curr. Drug Deliv.* **2015**, *12*, 192-199.
- [31] a) K. Oumzil, S. Khiati, M. W. Grinstaff, P. Barthélémy, *J. Control. Release* **2011**, *151*, 123-130; b) B. Wu, S. T. Lu, K. Deng, H. Yu, C. Cui, Y. Zhang, M. Wu, R. X. Zhuo, H. B. Xu, S. W. Huang, *Int. J. Nanomed.* **2017**, *12*, 6871-6882.
- [32] a) Z. Lin, H. Tian, F. Xu, X. Yang, Y. Mai, X. Feng, *Polym. Chem.* **2016**, *7*, 2092-2098; b) F. Mou, C. Chen, J. Guan, D. R. Chen, H. Jing, *Nanoscale* **2013**, *5*, 2055-2064.
- [33] a) A. Palanisamy, Q. Guo, *RSC Adv.* **2014**, *4*, 54752-54759; b) V. Haridas, A. R. Sapala, J. P. Jasinski, *Chem. Commun.* **2015**, *51*, 6905-6908.
- [34] J. S. Baek, C. C. Choo, N. S. Tan, S. C. J. Loo, *Oncotarget* **2017**, *8*, 80841-80852.
- [35] a) J. L. Markman, A. Rekechenetskiy, E. Holler, J. Y. Ljubimova, *Adv. Drug Deliv. Rev.* **2013**, *65*, 1866-1879; b) Q. Yin, J. Shen, Z. Zhang, H. Yu, Y. Li, *Adv. Drug Deliv. Rev.* **2013**, *65*, 1699-1715.
- [36] a) M. Eskandani, H. Hamishehkar, J. E. N. Dolatabadi, *DNA Cell Biol.* **2013**, *32*, 498-503; b) S. Ullah, M. R. Shah, M. Shoaib, M. Imran, A. M. A. Elhissi, F. Ahmad, I. Ali, S. W. A. Shah, *Drug Deliv.* **2016**, *23*, 3480-3491.
- [37] K. L. Nair, S. Jagadeeshan, S. A. Nair, G. S. V. Kumar, *J. Nanobiotech.* **2011**, *9*, 42.
- [38] R. Elumalai, S. Patil, N. Maliyakkal, A. Rangarajan, P. Kondaiah, A. M. Raichur, *Nanomedicine* **2015**, *11*, 969-981.

## Entry for the Table of Contents (Please choose one layout)

Layout 1:

## FULL PAPER

The cholesteryl lipoic acid conjugates have been exploited for the development of reduction responsive hollow non-phospholipid vesicles which showed concentration dependent spherical and triangular structures. In comparison to free doxorubicin, the vesicle encapsulated drug exhibited comparable and substantially high intracellular accumulation against drug sensitive and resistant cancer cells respectively, which offer an exciting strategy for the development of reduction responsive nanocarriers.



Krishan Kumar, Lalit Yadav,  
Paturu Kondaiah,\* and  
Sandeep Chaudhary\*

**Page No. – Page No.**

**Efficacious doxorubicin  
delivery using glutathione  
responsive hollow non-  
phospholipid vesicles  
bearing lipoyl cholesterol**

Layout 2:

## FULL PAPER

((Insert TOC Graphic here; max. width: 11.5 cm; max. height: 2.5 cm))

*Author(s), Corresponding Author(s)\**

**Page No. – Page No.**

**Title**

Text for Table of Contents